International Journal of GEOMATE, March, 2017, Vol 12, Issue 31, pp. 58-62
Geotec., Const. Mat. & Env., ISSN:2186-2990, Japan, DOI: http://dx.doi.org/10.21660/2017.31.6536

3D-FEM ANALYSIS OF SHIELD TUNNEL CONSTRUCTION WITH GROUND-SPRING MODEL

Pattanasak Chaipanna[1], *Pornkasem Jongpradist[1]

[1] Department of Civil Engineering, King Mongkut's University of Technology Thonburi, Thailand;

*Corresponding Author, Received: 15 June 2016, Revised: 15 August 2016, Accepted: 30 November 2016

ABSTRACT: The shield tunneling has been extensively implemented for construction of underground transportation systems in urban areas. Reports on tunnel segment damage during tunnel construction become increasing. The jack thrust force is the essential cause of damage to the segment. The objective of this article is to present the model which analyzes the behavior of tunnel lining during construction. The model consists of five rings and ten segments for each ring connected together with the shear springs which represent the segment joints and ring joints. The zero thickness interface elements are used to model the segment interface behavior and soil stiffness is represented by mean of ground springs. All relevant construction loads are taken into account in the analysis. The ground spring model is implemented into FEM program ABAQUS to analyze the behavior of segmental lining during construction along straight and curve alignments. The analysis results agree with the measurement data and confirm that the stresses of tunnel segments are governed by jack thrust force. The ground-spring model has been proven to be appropriate for analysis of behavior of the tunnel segments.

Keywords: 3D FEM, Soil-Tunnel Interaction, Ground spring model, and Tunneling construction

1. INTRODUCTION

The shield tunneling technology has been continuously developed with remarkable progress. The segmental lining is popularly used in the shield tunneling. The segments are sequentially erected as tunnel boring advances, which are consecutively coupled with the bolts in the longitudinal and circumferential directions of the tunnel. The packing materials are used between segments with the purpose of load distribution.

During the shield tunnel excavation, the tunnel linings are subjected to the construction loads, such as, the jack thrust, the shield tail pressure, the grouting pressure and ground pressure. Many reports of shield segment damage during construction have been increasingly presented and these indicate the significance of construction load [1], [2]. However, the conventional design of tunnel lining takes into account only the serviceability loads in shield tunneling [3], [4].

Nowadays, analysis of shield tunneling can be achieved by mean of three-dimensional (3D) model [5], [6]. These analyses take into account the steps of tunnel construction, but the tunnel lining is commonly modeled by means of continuous ring. Katebi et al.,[7] and Blom et al.,[8] model tunnel lining by segmental lining, but the surrounding soil is characterized by elastic medium which is not rational to represent the actual soil behavior.

Although, it is commonly realized that the effect of the tunnel construction loads on the tunnel lining must be taken into account in the analysis and design of shield tunnels, only few research has been carried out to grasp the effect of tunnel construction loads [5], [6]-[8]. This paper presents a three-dimensional analysis model to enhance the appreciation of tunnel lining behavior due to the construction loads. The reference case is referred to Nishin-Shinjuku [9] tunnel which allows the verification of the present analysis method.

2. REFERRENCE CASE AND FIELD MEASUREMENT

In order to verify the appropriateness of the present analysis, the field measured data during the construction of Nishin-Shinjuku tunnel have been used to validate the proposed model [9]. The Nishin-Shinjuku tunnel is a part of the Metropolitan Expressway Central Ring Shinjuku Line.

The Nishin-Shinjuku Tunnel comprises of twin tunnels and a total length of 600 m. The outer diameter of tunnel is 13.0 m, thickness is 0.55 m and segmental width is 1.2 m. For field instrumentation, strain gauges were installed in first three tunnel rings with 10 positions for each ring

Table 1 Soil properties used in analysis [9]

Earth layer	Value
Wet density (kN/m^3)	18.6
Adhesive force (kN/m^2)	38.0
Internal friction angle (deg)	37.0
Subgrade reaction coefficient (MN/m^3)	91.0
N value	50

The Nishin-Shinjuku Tunnel comprises of twin tunnels and a total length of 600 m. The outer diameter of tunnel is 13.0 m, thickness is 0.55 m and segmental width is 1.2 m. For field instrumentation, strain gauges were installed in first three tunnel rings with 10 positions for each ring.

The tunnel crown is located at the depth of 22 m while groundwater table is at 13 m below the ground level. The tunnel was excavated through very dense gravel and very dense sand. The geotechnical data are tabulated in Table 1.

3. ANALYSIS STRATEGY

This section presents a three-dimensional analysis for shield tunneling, which takes into account the soil and water pressures, the tail void grouting pressure, the wire brush grease pressure, the jack thrust and soil-tunnel interaction. The analysis is performed by means of FE analysis.

The tunnel lining considered in the analysis includes five rings, each ring comprises of ten segments, which are staggered alignment along the tunnel axis. The segments are coupled with the segment joints and ring joints in longitudinal and circumferential directions, respectively. These joints are considered using the shear spring elements. The assembly of tunnel lining is illustrated in Fig.1 (a). The attribution of packer material is represented with the interface element which involves the normal and tangential behaviors.

There are various loads acting on the tunnel lining, such as, jack thrust, wire brush pressure, tail void grouting pressure and earth pressure. These loads influence on the performance of the tunnel lining. For this reason, these loads are taken into account in the analysis, as seen in Fig.1 (b).

The soil-tunnel interaction is modeled by means of a series of radial springs [10], the stiffness of radial spring is regarded using nonlinear elastic behavior (Fig.2). The stiffness of radial springs are varied along the longitudinal tunnel, as seen in Fig.1(c).

The Ring1 in the model is only subjected by the jack thrust in longitudinal direction, no any loads acting on radial direction. The grease is injected into the gap between shield tail and the extrados of tunnel lining to prevent the external water flow into the shield. The grease pressure acts on the Ring2. Ring3 is subjected by tail void grouting pressure. The grout material is filled the gap between the extrados of tunnel lining and surrounding soil. The constant pressure is kept over the hydrostatic pressure of 90 kPa. Ring4 and Ring5 are subjected to the surrounding ground pressure which comprises the soil pressure and water pressure.

The simulation of shield tunneling is divided in two categories, the shield tunneling for straight forward alignment and the curve forward alignment. The hydraulic jack pattern for both categories are illustrated in Fig.3. The black circles are represented the active jack thrust, in the other hand, the white circles are represented the inactive jack thrust.

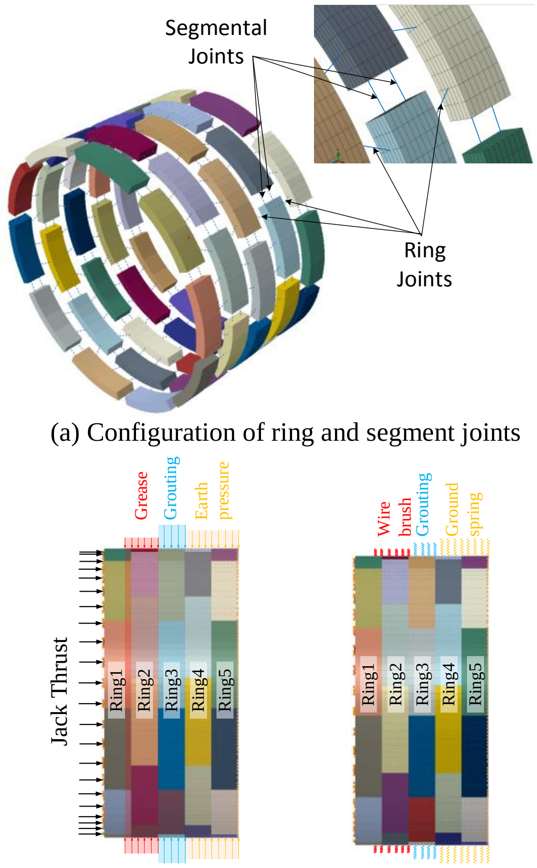

(a) Configuration of ring and segment joints

(b) Loads distribution (c) Radial springs

Fig. 1 Loads distribution and boundary condition of analysis model

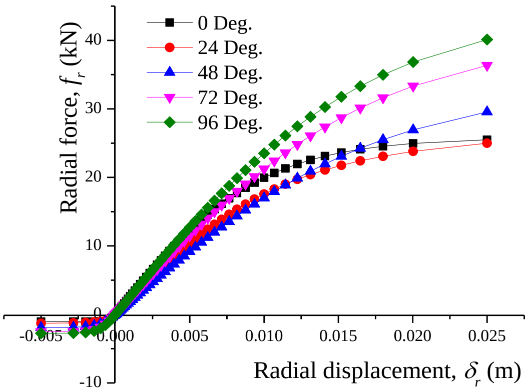

Fig. 2 Modeling of the soil-tunnel interaction

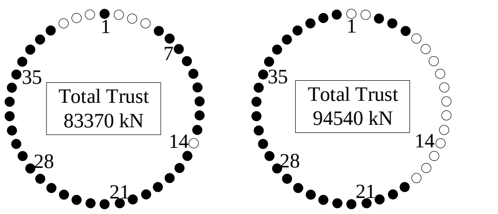

(a) Straight alignment (b) Curve alignment

Fig. 3 Configuration of jack thrust.

4. ANALYSIS RESULTS

The simulation results of Ring1, Ring2, and Ring3 are compared to the field measurements taken from literature to validate and calibrate this analysis method.

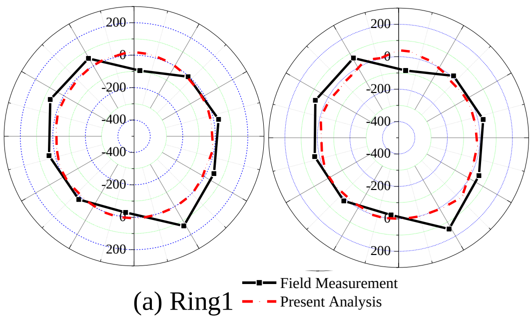

(a) Ring1

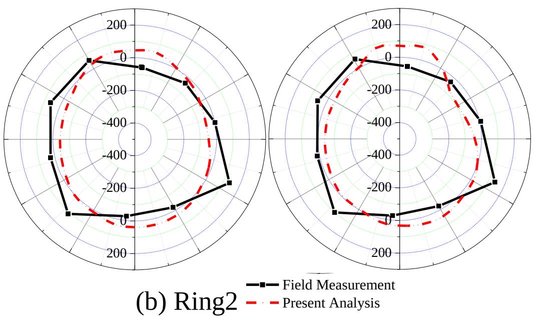

(b) Ring2

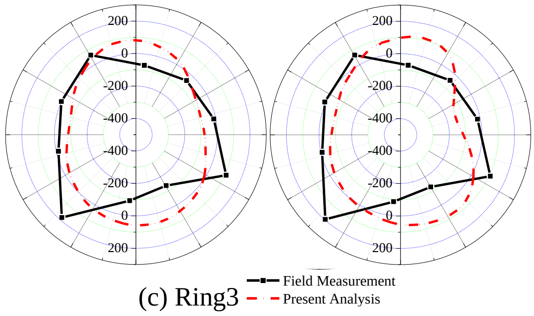

(c) Ring3

Fig.4 Comparison of bending moment (kN-m) between field measurement and present analysis (Left side for straight alignment and right for curve alignment).

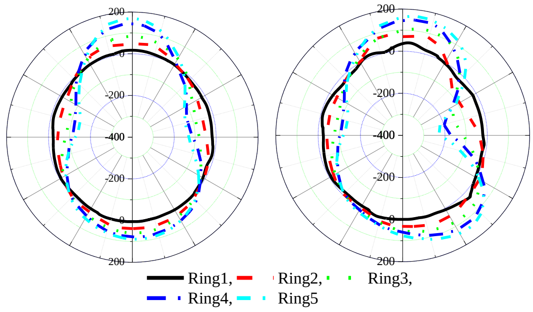

(a) Straight alignment (b) Curve alignment

Fig. 5 Computed bending moment distribution (kN-m).

The measured and analysis results from Figs.4 to 7 are traced from centerline of tunnel segments. The measured and computed results are compared by means of plotting the results (bending moment, forces and deformation) in the circumferential direction against the circumferential angle. The contour shedding of stress distribution are also depicted as illustrated in Figs.8 to 10.

Fig.4 shows the comparison between the measured and computed circumferential bending moments of the tunnel Ring1, Ring2 and Ring3. The left figures represent results of simulation during straight alignment, and the right figure is for shield tunneling during curve alignment. The circumferential bending moment occurs slightly in the Ring1 because there is no external force in circumferential direction; only gravitational force of the segments themselves exists. The jack thrusts are in longitudinal direction. The moment becomes increasing in Ring 2 and Ring 3 due to the grease and grouting pressures, respectively. Comparison between the computed and measured results reveal that the analysis can reproduce the moment distribution in a fair agreement with the measured ones. The difference between the straight and curve alignment can be also reflected.

Fig.5 summarizes the computed circumferential bending moments from all 5 rings. The maximum circumferential bending moment occurs in the Ring 5 as a result of different vertical and horizontal pressures of surrounding soil. The influence of jack thrust (as straight or curve alignment) on the bending moment is clearly seen as shown in Figs. 5(a) – (b).

Fig. 6 shows the distribution of circumferential force comparing between the measured and computed values. The maximum circumferential force appears in Ring2. For Ring 1 and Ring 2, it is seen that the computed forces are in good agreement with the measured one, whereas, the computed forces in Ring 3 are larger than those of the measurement.

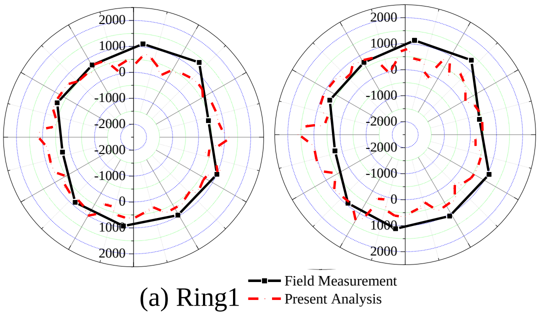

(a) Ring1

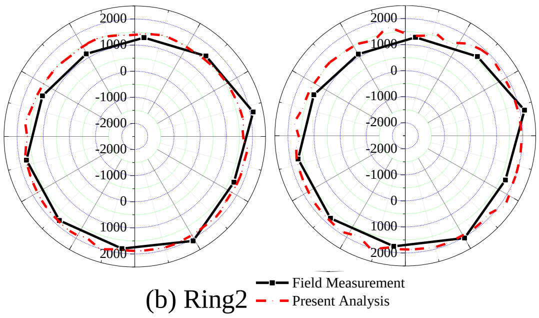

(b) Ring2

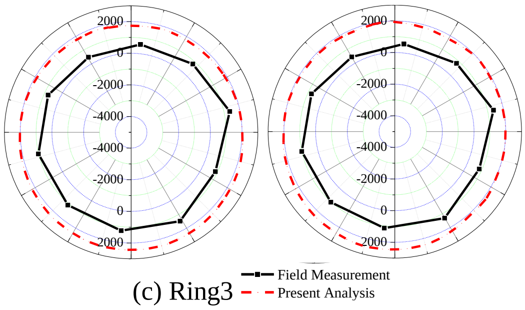

(c) Ring3

Fig. 6 Comparison of circumferential force (kN) between field measurement and present analysis (Left side for straight alignment and right for curve alignment).

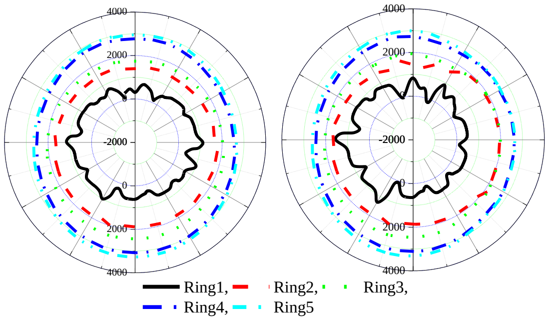

(a) Straight alignment (b) Curve alignment

Fig. 7 Computed circumferential force (kN).

From figs.4 and 6, it indicates that the analysis results satisfactorily correspond to the measurement for both bending moment and circumferential force. Fig. 7 depicts the computed circumferential forces from all 5 rings. The maximum circumferential load occurs at the invert of Ring 5. The jack thrust does not only affect the axial load, but also the circumferential load. Furthermore, a circumferential load of Ring5 is affected from the jack thrust too. The distribution of circumferential force of Ring 5 of straight alignment (Fig.7 (a)) differ slightly from that of curve alignment (Fig.7 (b)).

The distribution of the circumferential stress is shown in Figs.8 (a) to 8 (b) for straight and curve alignments, respectively. The jack thrust has strong influence on the circumferential stress. The circumferential stress mostly concentrated on the front face of Ring1 which is in accordance with the position of hydraulic jacks. The circumferential stress decreases in Ring2 and Ring3. The circumferential stress increases again in Ring4 and Ring5 due to radial pressure. The eccentric jack thrust obviously shows the difference of stress intensity between the straight and curve alignment. The jack thrust directly affects to the longitudinal stress, this stress concentrates at the hydraulic jack position on the front face of Ring1. The longitudinal stress gradually decreases in the other rings. The contour shading of longitudinal stress of straight and curve alignments obviously differ as seen in Figs.9 (a) to 9 (b).

The computed shear stress distribution in tunnel lining is shown in Figs.10 (a) to 10 (b). Due to the tunnel lining is segmental, the shear stress of adjacent segments are transferred by mean of interface elements and tunnel joints. The maximum shear stress occurs at the position of hydraulic jack.

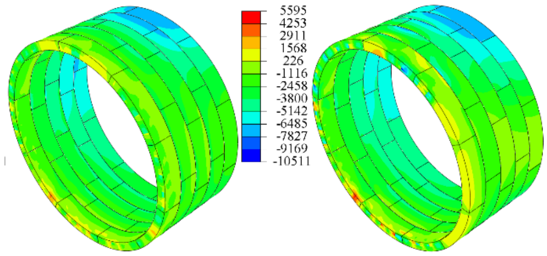

a) Straight alignment b) Curve alignment

Fig. 8 Distribution of circumferential Stress (kPa).

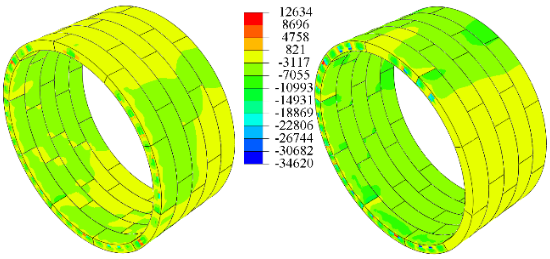

a) Straight alignment b) Curve alignment

Fig. 9 Distribution of longitudinal stress (kPa).

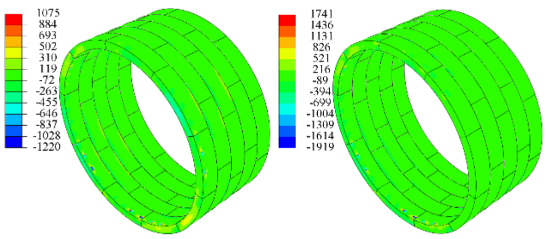

a) Straight alignment b) Curve alignment

Fig. 10 Distribution of shear stress (kPa).

5. CONCLUSION

A three-dimensional analysis of shield tunnel segments during construction has been presented, which takes into account all relevant interactions and loads, i.e., soil and water pressures, the grouting pressure, the jack thrust force and the grease pressure. The conclusions from this study are as follows:

- The present analysis satisfactorily correspond to the field measurement of case study.
- The analysis results can reproduce the influence of jack thrust on the tunneling behavior.
- The jack thrust influence on both displacement and structural forces of tunnel lining.
- The jack thrust is the main cause of the maximum stress in the segment. Therefore, the internal stress of tunnel lining is governed by the jack thrust.

6. REFERENCES

[1] Sugimoto, M., "Causes of Shield Segment Damages During Construction", in Proc. Int. Symp. On Underground Excavation and Tunnelling, Bangkok, 2006,Thai, pp.67-74.

[2] Wu M.Q., "Application study on steel fiber concrete segment in metro tunnel engineering", Guangdon Building Materials 3, 2004, pp.6-8.

[3] ITA-WG2, "Guidelines for the Design of Shield Tunnel Lining", Tunnelling and Underground Space Technology, Vol.15, No.3, 2000, pp.303-331.

[4] Japanese Society of Civil Engineerings (JSCE), "Japanese Standard for Shield Tunneling", 3rd ed. 1996, Tokyo, Japan.

[5] Kasper T. and Meschke G., "A 3D finite element simulation model for TBM tunnelling in soft ground", Int. J. Numer. Anal. Meth. Geomech. 28, 2004, pp.1441-1460.

[6] Katebi H., Rezaei A.H., Hajialilue-Bonab M. and Tarifard A., "Assessment the influence of ground stratification, tunnel and surface buildings specifications on shield tunnel lining loads (by FEM)", Int. J. Tunn. Undergr. Space Techno. 49, 2015.

[7] Blom C.B.M., van der Horst E.J. and Jovanovic P.S., "Three-dimensional Structural Analyses of the Shield-Driven Green Heart Tunnel of the High-Speed Line South", Int. J. Tunn. Undergr. Space Techno. 12, 1999, pp. 217-224

[8] Mo H.H. and Chen J.S., "Study on inner force and dislocation of segments caused by shield machine attitude", Int. J. Tunn. Undergr. Space Techno. 23, 2008, pp.281-291.

[9] Tajima M., Kishida M., Fukai N. and Saitou M., "Study on shield tunnel construction loads using a three-dimensional FEM model", in Proc. Tunnel Engineering, JSCE Vol.14, 2004, pp.353-360.

[10] Chaipanna P., Jonpradist P. and Kalasin T., "3D FEA of Shield Segmental Lining with Ground Spring Model", in Proc. ITA-AITES World Tunnel Congress 2012, pp.114-121.